CellPress

Cell Chemical Biology

Review

2′-OH as a universal handle for studying intracellular RNAs

Lu Xiao,[1] Linglan Fang,[1] and Eric T. Kool[1,2,*]
[1]Department of Chemistry, Stanford University, Stanford, CA 94305, USA
[2]Sarafan ChEM-H, Stanford University, Stanford, CA 94305, USA
*Correspondence: kool@stanford.edu
https://doi.org/10.1016/j.chembiol.2023.10.022

SUMMARY

RNA plays pivotal roles in most cellular processes, serving as both the traditional carrier of genetic information and as a key regulator of cellular functions. The advent of chemical technologies has contributed critically to the analysis of cellular RNA structures, functions, and interactions. Many of these methods and molecules involve the utilization of chemically reactive handles in RNAs, either introduced externally or inherent within the polymer itself. Among these handles, the 2′-hydroxyl (2′-OH) group has emerged as an exceptionally well-suited and general chemical moiety for the modification and profiling of RNAs in intracellular studies. In this review, we provide an overview of the recent advancements in intracellular applications of acylation at the 2′-OH group of RNA. We outline progress made in probing RNA structure and interactomes, controlling RNA function, RNA imaging, and analyzing RNA-small molecule interactions, all achieved in living cells through this simple chemical handle on the biopolymer.

INTRODUCTION

Decades of study have revealed that intracellular RNAs connect with most functions of the cell. Coding and non-coding RNAs (ncRNAs) have crucial roles from gene translation to regulation of many cellular processes in normal and pathological conditions.[1,2] The versatile structures, high dynamics, and pervasive locations enable RNAs to efficiently modulate cell functions and adapt to environmental changes.[3] Although the complexity of the transcriptome is becoming increasingly appreciated and delineated, many RNA-related mechanisms and structure-function relationships remain unknown.[4] In addition, beyond basic science, the number of RNAs developed to treat diseases and exploited as vaccines is rapidly growing.[5,6] Understanding RNA structures, interactions, dynamics, and functions in cells is critical for their optimal applications as engineered drugs, cellular devices, therapeutic targets, and tools for synthetic and molecular biology.[7,8] Thus, deep analysis of RNA structure, function, and its interactome is important both for basic science and biomedical applications.

Recently, a range of novel chemical technologies, often employed in conjunction with deep sequencing, have been developed to illuminate unanswered questions in the transcriptome. Many of the technologies either introduce novel chemical handles into RNAs or take advantage of the existing ones (*e.g.*, nitrogens on bases, 2′-hydroxyl groups on ribose sugars). Chemical or enzymatic labeling of RNA with modified nucleotides has been used to study cellular kinetics, dynamics, and locations.[9,10] Crosslinking technologies, such as UV or chemical crosslinking and immunoprecipitation (CLIP), react with native RNA nucleotides or use modified nucleobases to study RNA interactions.[11,12] Photoreactive diazirine groups have similarly been employed to investigate interactions.[13,14] Chemical probing approaches, including dimethyl sulfate (DMS) footprinting,[15] N_3-kethoxal probing with deep sequencing (Keth-seq),[16] and selective 2′-hydroxyl acylation analyzed by primer extension (SHAPE),[17] all employing the reaction of distinct functional groups in RNA, have been established for transcriptome-wide RNA structure mapping. All of these (except certain photocrosslinking methods) involve the reaction of electrophilic molecules with nucleophiles in RNA; DMS and kethoxal probing involve reactions at specific nucleic acid bases and provide selectivity for unpaired nucleobases or paired ones. The third electrophilic chemical approach, acylation, is distinct by involving the 2′-hydroxyl group on the nucleotides rather than the bases.

We suggest that an ideal chemical handle for probing RNA will exhibit a number of properties, including presence all along the RNA strand, responsiveness to RNA structure, and the ability to be addressed chemically both *in vitro* and in living cells. Based on these criteria, the 2′-hydroxyl (2′-OH) is arguably a near-ideal chemical handle for modifying and profiling RNA, given that almost every nucleotide possesses a 2′-OH group, regardless of sequence. The 2′-OH group in RNAs acts as a nucleophile with higher reactivity than most alcohols.[18] This increased reactivity is attributed to a lower pKa (~12.5) that promotes transient oxyanion formation at the 2′-OH group as a result of inductive effects of nearby oxygen and nitrogen atoms.[19] Multiple chemical modification reagents and methods specific to the 2′-OH group are now applicable to RNAs both *in vitro* and *in vivo*.[20] Recent kinetics studies of mono- and dinucleotides further established that acylation at the 2′-OH position, at least for reagents studied to date, is considerably more efficient than reaction at

the 5′-OH or exocyclic amines.[21,22] This selective reactivity forms the basis for employing 2′-OH acylation for RNA studies. Acylations can be performed in trace yields for structure mapping, and with optimized reagents, in high yields for stoichiometric applications.[20] The expanding reagent catalog for RNA 2′-OH modification enhances the potential of using 2′-OH group to study intracellular RNAs.

Previous reviews have discussed the use of trace-level acylation at 2′-OH for probing secondary structure via the primer extension method (SHAPE) originated by Weeks, most often applied to extracted or *in vitro* transcribed RNAs.[23,24] Here, we will focus on intracellular applications of acylation at the 2′-OH group of RNA, which requires specialized reagents that are cell permeable and have extended lifetimes (Table 1). Applications include both trace-level mapping and probing strategies, as well as high-yield acylations for modification, conjugation, and stabilization of the biopolymer. We will also summarize recent insights into RNA structure, interactions, regulation, imaging, and profiling of small molecule interactions gathered with the help of new 2′-OH-targeting reagents and methods.

2′-OH GROUP AS A HANDLE FOR RNA STRUCTURE MAPPING BY CELL-PERMEABLE SHAPE REAGENTS

RNA folds into structures that range from simple stem-loop configurations to complex tertiary structures and further quaternary assemblies with ribonucleoproteins. The functions of RNAs are often modulated by structural changes in response to diverse cellular environments.[3] Importantly, disruptions of RNA structure have been linked to human diseases.[3,25] For example, disease-associated single-nucleotide polymorphisms can induce changes in RNA structure, assembly, and embedded mechanisms, leading to pathological phenotypes. Therefore, methods are needed to probe RNA structures and their conformational dynamics in the cell to improve our understanding of mechanisms for RNA function. 2′-OH acylation has been widely applied to RNA structure analysis using SHAPE chemistry.[26,27] The chemistry is based on a simple reaction between the reactive carbonyl center of probing reagents with the 2′-OH groups in RNAs (Figure 1A). The 2′-OH reactivity is governed by local nucleotide accessibility arising from conformational constraints and dynamic flexibility.[28,29] Pioneering work done by the Weeks group revealed that RNA 2′-OH acylation *in vitro* by isatoic anhydrides (e.g., NMIA and 1M7) stalls reverse transcriptase (RT) during complementary DNA (cDNA) synthesis.[17,30] As reverse transcriptase stops one nucleotide before an acylated nucleotide, the primer extension yields different lengths of cDNAs, which can be analyzed by electrophoresis (Figure 1B). Weeks and colleagues reported initial studies of several *in vitro* RNA structures via scarce acylation of NMIA and 1M7, such as $tRNA^{Asp}$ and the *Escherichia coli* 16S ribosomal RNA (rRNA),[31] demonstrating the feasibility of SHAPE chemistry in mapping RNA structures. Later, Lucks et al. coupled SHAPE chemistry with high-throughput sequencing (SHAPE-seq), further broadening the application of the SHAPE method.[32]

In-cell structure mapping of specific RNAs

Encouraged by the early acylation-based studies of *in vitro* RNA structures, new SHAPE reagents were developed for cellular RNA analysis (Figure 1B), making use of reagents with longer aqueous lifetime and improved cell permeability. The acylimidazole reagents FAI and NAI (Figure 1A) resulted in enhanced RNA intracellular acylation signals that enabled efficient structure probing. In 2013, Spitale et al. probed intracellular RNA structures with FAI and NAI in living mammalian, bacteria, and insect cells.[33] The data, analyzed by electrophoresis, showed robust rRNA structure folding and revealed the location of RNA-RNA and RNA-protein contacts by comparing *in vitro* and *in vivo* SHAPE experiments. More recently, Ding and colleagues employed the NAI chemical probing method with high-throughput sequencing to interrogate transcriptome-wide RNAs in plants.[34] They developed a CAP-STRUCTURE-seq method to capture the intact mRNA structurome in *Arabidopsis thaliana*. By analyzing the RT stops profile caused by NAI acylation, the results revealed the regulatory mechanism of mRNA structure in microRNA cleavage. In addition, as NAI displayed preferential modification of the last G in folded RNA G-quadruplexes leading to RT stops, Yang et al. applied the method SHALiPE-Seq to detect RNA G-quadruplexes in the *Arabidopsis* transcriptome and indicated their regulatory roles in plant growth.[35]

In addition to RT-stop mapping, mutational profiling (termed SHAPE-MaP) emerged, taking advantage of mutations introduced during reverse transcription past acyl adducts[36] (Figure 1B). The processivity of reverse transcriptase can be adjusted by replacing standard Mg^{2+} with a high concentration of Mn^{2+} as the only divalent ion in RT buffers,[36,37] enabling an RT to bypass acyl adducts rather than stop. This leads to distinct mutational profiles that indicate acylation. Both anhydrides (*e.g.*, 1M7) and acylimidazole reagents (*e.g.*, FAI, NAI) (Figure 1A) can be employed for the MaP method, showing similar mutational patterns with NAI and FAI displaying a slightly increased mutational frequency (~1%) likely due to the size and shape of adducts.[38,39] This approach can identify multiple mutations in a single transcript, enabling single-molecule analysis and interaction correlation studies.[27,40,41] For example, employing the anhydride 1M7, Weeks et al. reported the structure domain of Xist lncRNA that governs specific protein interactions in mouse trophoblast stem cells.[42] They further studied the diversity of endogenous mRNA structures involving translation in *E. coli* cells.[43] More recently, the Incarnato group utilized the SHAPE mutational signal derived from NAI to map the secondary structure of the full SARS-CoV-2 coronavirus genome in living infected Vero E6 cells.[44] The study showed the conserved sequence region of SARS-CoV-2 and structure covariation with other coronaviruses and provided a structure model for identifying putative druggable pockets. The Wan and Huber groups conducted a relevant study on mapping SARS-CoV-2 virus-host interactions using similar NAI acylation probing.[45] Other classes of RNA structure, such as circular RNAs, have also been investigated with NAI probing combined with mutation profiling in living cells.[46] Different from mapping average RNA structures, methods have also been developed to study RNA isoform structures via SHAPE mutational profiles. In 2021, the Wan and Nagarajan groups developed "PORE-cupine" to disclose isoform-specific RNA structures in human embryonic stem cells transcriptome, using RNA 2′-OH group as a chemical probing handle along with long-read nanopore sequencing.[47] In 2022, Ding and coworkers utilized single-molecule-based RNA

Table 1. Summary of reagents, terms, and methods using 2′-OH group as a handle for RNA analysis

Application	Reagent	Half-life	Approach	Reference
RNA structure mapping	NMIA	260 s at 37°C	SHAPE (RT-stop)	Merino et al. 2005[17]
	1M7	17 s at 37°C	SHAPE (RT-stop)	Mortimer et al. 2007[30]
			SHAPE-seq (RT-stop)	Lucks et al. 2011[32]
			SHAPE-MaP (RT-mutation)	Smola et al. 2016[42]; Mustoe et al. 2018[43]
	FAI	73 min at 25°C	SHAPE (RT-stop)	Spitale et al. 2013[33]
	NAI	33 min at 25°C	SHAPE (RT-stop)	Spitale et al. 2013[33]
			CAP-STRUCTURE-seq (RT-stop)	Yang et al. 2020[34]
			SHALiPE-Seq (RT-stop)	Yang et al. 2020[35]
			SHAPE-MaP (RT-mutation)	Manfredonia et al. 2020[44]; Yang et al. 2021[45]
			smStructure-seq (RT-mutation)	Yang et al. 2022[48]
	NAIN3	~30 min at 25°C	icSHAPE (RT-stop)	Spitale et al. 2015[49]; Sun et al. 2019[50]; Sun et al. 2021[51]
			icSHAPE-MaP (RT-mutation)	Luo et al. 2021[52]; Wang et al. 2021[53]
			PORE-cupine (RT-mutation)	AW et al. 2021[47]
	2A3	260 min at 25°C; 60 min at 37°C	SHAPE-MaP (RT-mutation)	Marinus et al. 2021[54]
	PyIm	30 min at 25°C; 8 min at 37°C	SHAPE-MaP (RT-mutation); SHAPE (RT-stop)	Marinus et al. 2021 (54); Xiao et al. 2023[56]
	AcIm	3 min at 37°C	SHAPE-MaP (RT-mutation); SHAPE (RT-stop)	Stephenson et al. 2022[57]; Xiao et al. 2023[56]
RNA interaction capture	BINARI	/	Crosslink	Velema et al. 2020[58]
	TBIA	30 s/180 s at 37°C	SHAPE-JuMP	Christy et al. 2021[60]
	DPI	5 min at 25°C	SHARC-exo	Damme et al. 2022[59]
RNA caging and on-demand activation	NAIN3	~30 min at 25°C	RNA cloaking	Kadina et al. 2018[66]; Habibian et al. 2019[67]; Wang et al. 2020[68]
	Azido quinone methide (QM)	/	RNA cloaking	Park et al. 2021[69]
	Photocloaking agent (PCA)	/	RNA photocloaking	Velema et al. 2020[21]
Site-directed RNA labeling	NAIN3	~30 min at 25°C	RAIL; TRAIL	Xiao et al. 2020[80]; Xiao et al. 2021[81]
	DNAzyme or Ribozyme	/	Enzymatic labeling	Buttner et al. 2014[82]; Maghami et al. 2019[84]; Maghami et al. 2020[83]
Profiling small molecule interactions	1M7	17 s at 37°C	SHAPE; SHAPE-MaP	Wang et al. 2008[85]; Zeller et al. 2022[86]; Zeller[87]
	Lev-AI (drug + acylimidazole)	/	RBRP	Fang et al. 2023[94]
	Coumarin derivative probe	/	cgSHAPE	Tang et al. 2023, bioRxiv[95]

structure sequencing (smStructure-seq), generating the SHAPE reactivity based on NAI-adduct mutational profiles to study the isoforms of non-coding RNAs in *Arabidopsis*.[48] This work demonstrated that the isoforms adopt diverse and dynamic structure conformations with relevant functions in response to external conditions.

Transcriptome-wide mapping

Although reagents in conjunction with deep sequencing provide useful intracellular RNA structural information on an RNA-by-RNA basis, there remain some obstacles to obtaining information on a transcriptome-wide basis. RNA acylation is performed under single-hit kinetics with ~1 modification per 300

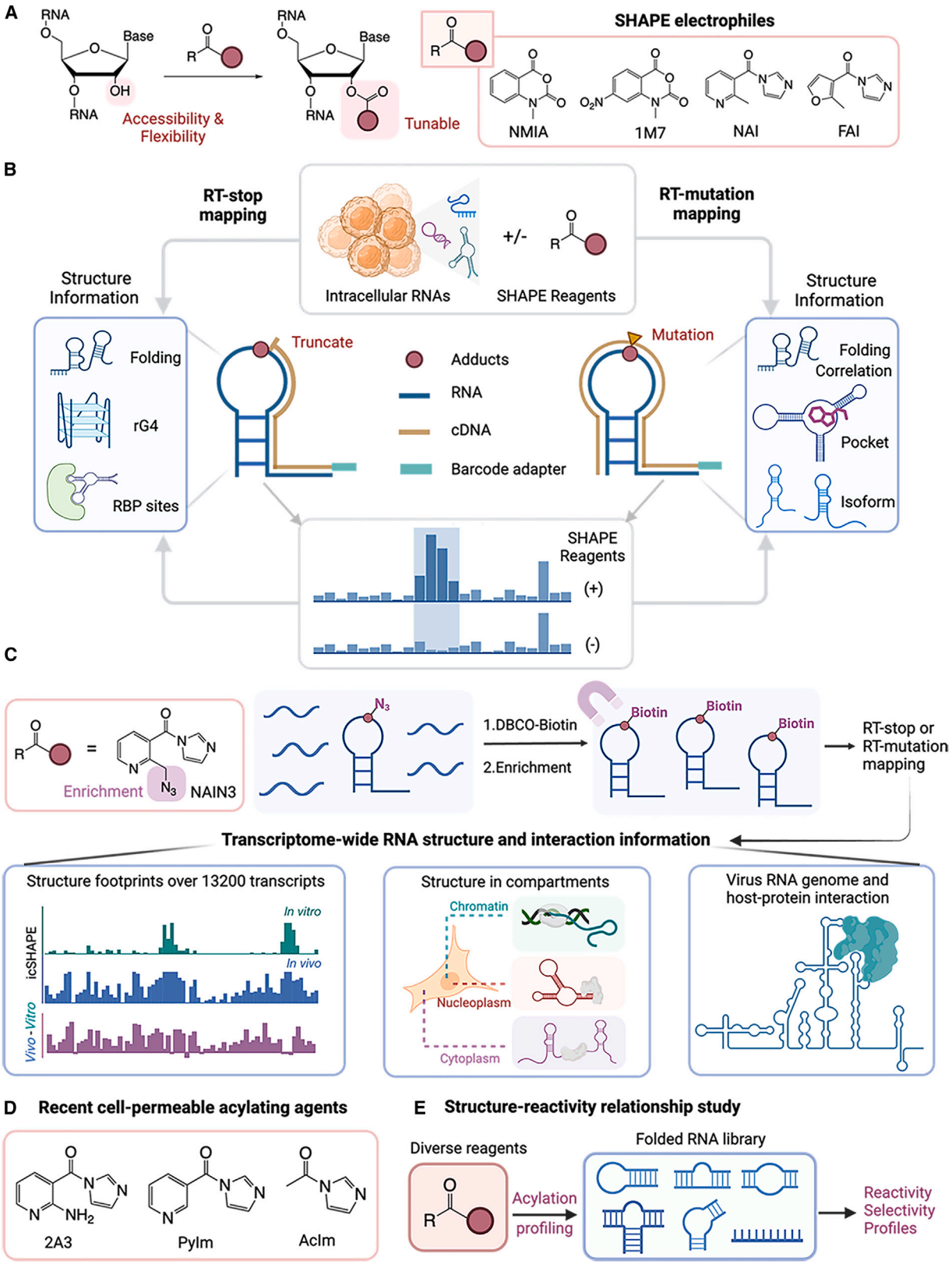

(legend on next page)

nucleotides to yield useful data.[20,39] Therefore, only a small fraction (~10–15%) of all RNAs are actually modified, resulting in the RT-stop or mutation sites being diluted by a large number of other stops due to RT fall-off and RNA fragmentation, wasting sequencing reads. To address this, the compound NAI was modified with an azido group resulting in reagent NAIN3, which enables the probing of RNA structures with enrichment of adduct-forming sites by clicking on a biotin group (Figure 1C). By analyzing the resulting RT-stop profile, this reagent was used to measure the intracellular structures of 13,200 polyadenylated RNAs in mammalian cells via the *in vivo* click SHAPE (icSHAPE) method.[49] It can also identify protein-binding sites and m^6A epitranscriptomic modifications by analyzing the difference in RT-stop profiles between different conditions. Subcellular compartment-specific RNA structures were studied later with icSHAPE using NAIN3 reagent, examining the cellular RNA structures in chromatin, nucleoplasm, and cytoplasm.[50] In 2021, Sun et al. applied the icSHAPE method to map *in vivo* SARS-CoV-2 RNA and identified host-binding proteins that can be targeted by repurposed FDA-approved drugs.[51] In conjunction with icSHAPE enrichment strategy and mutational analysis (icSHAPE-MaP) using NAIN3, more RNA structure-function correlations have also been discovered during intracellular processes.[52,53]

Since acylation of 2′-OH groups has become widely useful for RNA structure mapping, more studies on cell-permeable acylating reagents have been carried out to expand the catalog of probing tools and to understand structure-reactivity relationships for more accurate RNA structure analysis.[29,54,55] Incarnato and colleagues have introduced a new probe, 2-aminopyridine-3-carboxylic acid imidazolide (2A3), (Figure 1D) displaying improved performance for *in vivo* RNA structure prediction via mutation profiling, particularly in bacteria, possibly due to increased cell permeability.[55] Kool and colleagues developed a profiling strategy to survey the reactivity and selectivity of diverse acylating reagents in "generic" RNA libraries containing varied secondary structure motifs with homogeneous loops[29,56] (Figure 1E). The profiling data revealed varied acylation reactivity patterns among different unpaired motifs and substantial effects of reagent structure on acylating RNA 2′-OH groups. The physicochemical features of reagent structures and local structural constraints of RNAs together gated the access of the reagent carbonyl group to specific 2′-OH groups, thus providing additional considerations in accurate analysis of RNA structures via SHAPE. Among the screened acylating reagents, pyridyl acylimidazole (PyIm) and acetylimidazole (AcIm) (Figure 1D) showed high loop-stem selectivity and more balanced reactivity along loops. Both reagents are cell permeable and can react with rRNAs in intact mammalian cells within 5 min resulting in efficient RT stops[56] or RT mutations.[55] Pyridyl acylimidazole performed similarly as it probed RNAs in living bacteria cells,[55] while notably, acetylimidazole displayed a striking ability to map intracellular rRNAs structures underlying associated ribosomal proteins, most likely due to the small size. In related work, Weeks and coworkers recently showed that acetylimidazole, applied *in vitro*, can be employed for full-length single-molecule SHAPE analysis by nanopore sequencing.[57] The last two observations suggest that acetylimidazole (AcIm) in particular has significant potential for broader intracellular RNA analysis.

CROSSLINKING 2′-OH GROUPS: CAPTURE OF LOCAL AND TRANSIENT INTERACTIONS IN CELLS

The dynamic interactions between RNAs play crucial roles in regulating diverse cellular processes.[3] As a result, comprehensive characterization of these interactions in their native cellular context remains highly desirable. Among developed methodologies, chemical crosslinking of RNA is one of the most widely used approaches to investigate RNA interacting components, dynamic contacts, and spatial assembles inside cells.[12] This strategy employs defined small-molecule crosslinkers to capture interacting species, followed by identification of crosslinked nucleotides via deep sequencing. Many chemical crosslinker molecules have been utilized; these reagents can crosslink different reactive sites of RNAs by exogenous addition or internal installation in RNA scaffolds prior to crosslinking.[12] For example, psoralen and its derivatives crosslink pyrimidines in RNA duplexes upon 365 nm UV irradiation and reverse upon exposure to 254 nm light; similarly, diazirine and derivatives incorporated on RNA nucleobases crosslink functional groups upon photolysis by forming highly reactive carbenes.[13] Distinct from those previous approaches, crosslinking at the 2′-OH position in RNAs offers the possibility of providing links that are not dependent on specific nucleobases, thus potentially offering more comprehensive coverage and a lack of nucleotide bias.

Since RNA acylation is achieved with an activated carbonyl group, two consecutive acylations with bifunctional compounds should form a crosslink between nearby ribonucleotides (Figure 2A). Velema et al. investigated this possibility by designing bisnicotinic azide reversible interaction (BINARI) probes (Figure 2B), which contained two electrophilic moieties that can acylate 2′-OH groups of spatially proximal nucleotides, resulting in a covalent crosslink between interacting RNA strands.[58] The two functional moieties were bridged via polyethylene glycol spacers, whose varied lengths displayed significant effects on the crosslinking efficiency, ranging from 45% to 84% between

Figure 1. Reactions at 2′-OH in RNA as a structure mapping strategy

(A) Schematic of the acylation reaction involving a 2′-hydroxyl (2′-OH) group and an activated carbonyl, serving as the basis for SHAPE measurement. The appended group (red) is varied and tuned for different types of SHAPE electrophiles.

(B) Schematics of in-cell SHAPE mapping to identify probe adducts via reverse transcription (RT) stops or RT mutations. Diverse SHAPE strategy can learn various structure information, including folding and correlation, specific structure (e.g., RNA quadruplex (rG4)), RNA-protein interaction (e.g., RBP sites), and RNA isoforms.

(C) Schematics of chemical approaches to enrich modified sites for transcriptome-wide RNA study. Combining with enrichment assay, a larger set of intracellular RNAs and their interactome can be analyzed.

(D) Chemical structure of recently developed cell-permeable acylating reagents.

(E) Strategy of studying structure-reactivity relationship of diverse acylating reagents and different RNA secondary structure motifs for improved intracellular RNA structure mapping.

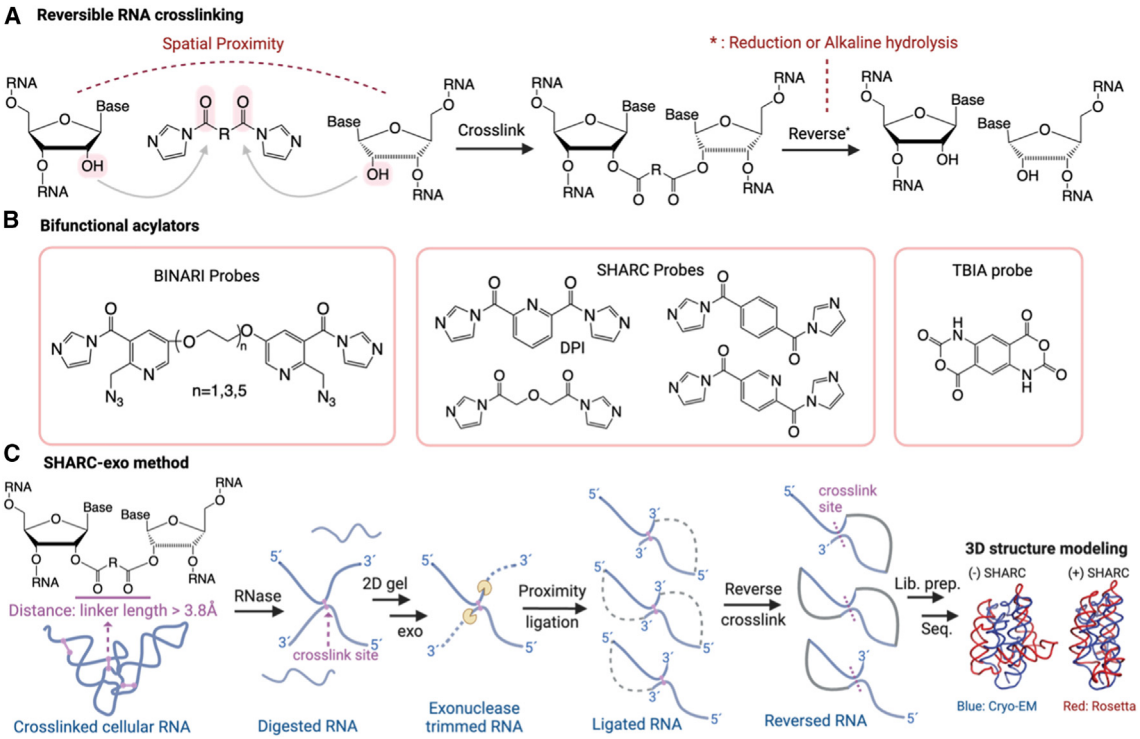

Figure 2. Structures and applications of crosslinkers for RNA 2′-OH groups

(A) Chemical mechanism of reversible RNA crosslinking via double-acylation of proximal 2′-OH groups with bifunctional reagents.

(B) Molecular structures of bifunctional acylators.

(C) Schematics of integrated Spatial 2′-Hydroxyl Acylation Reversible Crosslinking (SHARC-exo) method[59] for intracellular RNA 3D structure. Varied lengths of bifunctional acylators are employed to measure RNA 3D distance via reversible crosslinking, exonuclease (exo) trimming, proximity ligation, library preparation and high-throughput sequencing. Analysis of spatial distances among nucleotides in an RNA enables 3D structure modeling.

two hairpin RNAs. The crosslink could be released by phosphine-mediated reduction, which enabled the analysis of individual RNA components without interference. Subsequently, the Lu and Velema groups applied other bifunctional acylators to capture RNA-RNA contacts for 3D structure determination.[59] They developed a method termed spatial 2′-hydroxyl acylation reversible crosslinking (SHARC) by utilizing crosslinking acylators with defined lengths to measure the 3D distance between nucleotides of intracellular RNAs (Figures 2B and 2C). The crosslinking of the nearby RNA 2′-OH groups achieved 97% efficiency with dipicolinic acid imidazolide (DPI) reagent and was reversed by borate buffer (pH 10.0) without apparent RNA damage. After crosslinking, cellular RNAs were isolated and trimmed by exonuclease (exo), followed by proximity ligation and high-throughput sequencing to identify crosslinking sites. The spatial distances between the crosslinked 2′-OH groups of nucleotides were determined by linker length and RNA structure flexibility. By incorporating the SHARC-exo distance data into Rosetta-based 3D modeling, the resolution of RNA structure was improved to near nanometer resolution. By integrating SHARC-exo with PARIS and CLIP methods, the authors demonstrated the compact folding of 7SK RNA, revealing the structural basis of functions for this critical transcription regulator. These results also established a strategy for measuring RNA 3D structure and alternative conformation in native cellular contexts.

Recently, Weeks and colleagues designed another bifunctional acylating reagent, *trans*-bis-isatoic anhydride (TBIA), containing two electrophilic isatoic anhydride moieties to crosslink nearby 2′-OH groups[60] (Figure 2B). Although not yet tested in cells, this reagent holds the potential to study intracellular RNA 3D structure in combined with a crosslink-traversing reverse transcriptase.

2′-OH GROUP AS A TARGET FOR RNA CAGING AND ON-DEMAND ACTIVATION IN CELLS

Caging RNAs for on-demand cellular activation has been widely studied and employed for switching on RNA interference and mRNA translation.[61,62] Methods to cage RNAs are primarily based on introducing blocking modifications to the reactive sites of RNA.[63] Notably, the 2′-OH group reaction of RNA has been studied since 1965, showing the loss of biological function after high-level acetylation of tRNA.[64] Although this acetylation was not reversible, the results indicate the potential to regulate RNA functions via the 2′-OH group. In 1998, Chaulk and MacMillan demonstrated that the 2′-OH group could be used to cage a ribozyme.[65] The photosensitive caging group ortho-2-nitrobenzyl was incorporated into a hammerhead ribozyme via solid-phase synthesis. The caged *in vitro* RNA-cleaving reactivity was recovered upon UV photolysis, establishing the 2′-OH group as an effective site for caging, albeit not by acylation. Distinct from total synthesis, acylation provides a post-synthetic modification of RNA that can be performed in one step and can be applied to RNA of any length or origin. This can make caging

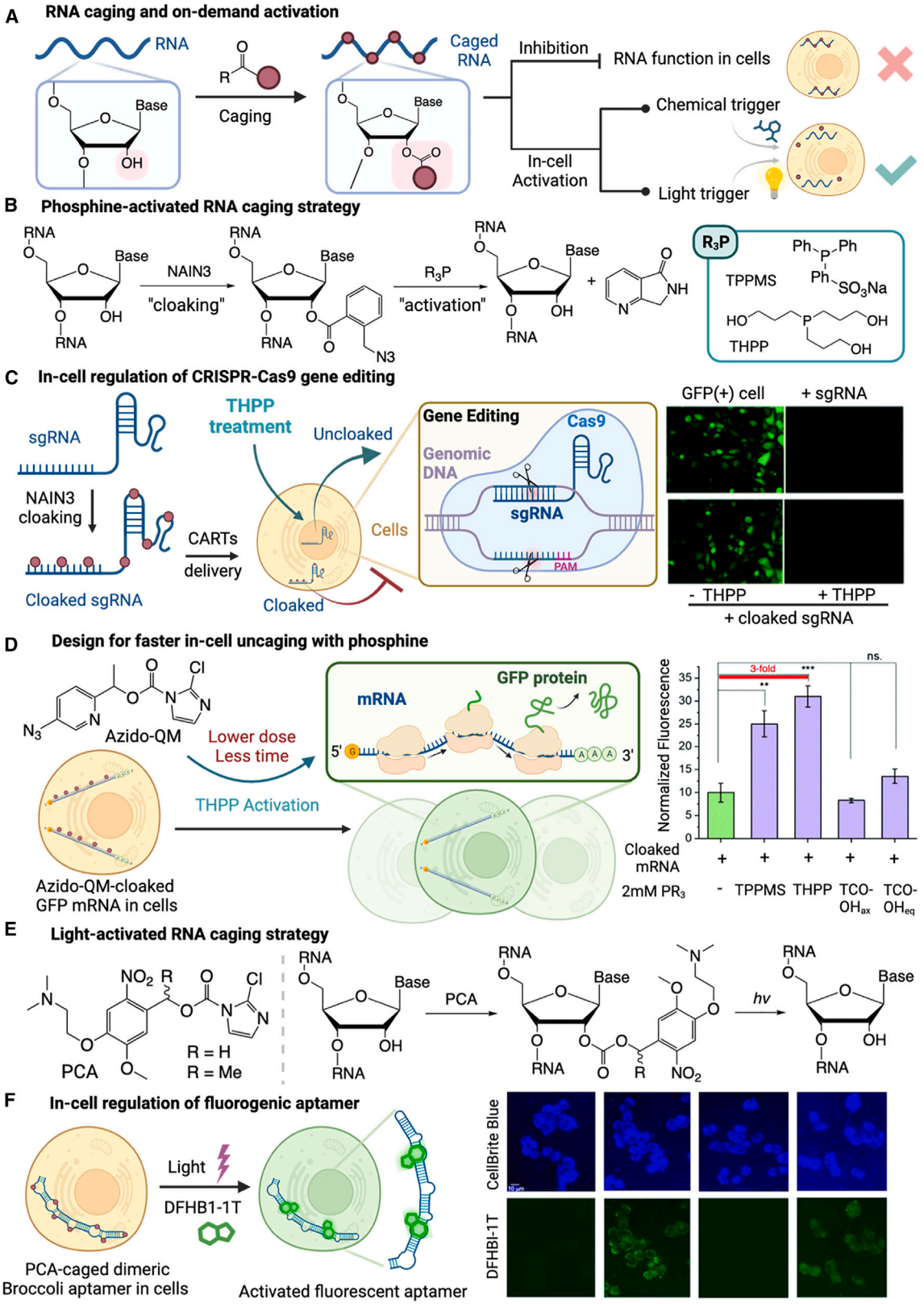

(legend on next page)

accessible to laboratories that do not possess solid-phase RNA synthesis chemistry expertise.

The potential of 2′-OH acylation for caging has been explored by designing chemical and optical strategies applied in cells for on-demand activation (Figure 3A). The previously developed water-soluble nicotinyl acylating agent NAIN3 shows trace-level RNA reactions for transcriptome structure probing, but due to its high solubility and extended half-life, it can also acylate RNA at stoichiometric levels. To take advantage of this, Kietrys et al. employed NAIN3 to poly-acylate ("cloak") RNA for activity caging[66] (Figure 3B). To restore RNA function, the azido group can be reduced to an amine by water-soluble phosphines, releasing the restored RNA molecule by intramolecular lactam formation. Testing this with a fluorescence-generating RNA aptamer, they showed >95% caging ability by NAIN3 and revealed complete recovery by treating with 5 mM diphenylphosphinoethylamine for 1h. Two laboratories later applied this reversible RNA acylation method using NAIN3 to control CRISPR-Cas9 gene editing in living cells[67,68] (Figure 3C). Habibian et al.[67] cloaked the CRISPR single guide RNA (sgRNA) targeting the gene of green fluorescent protein (GFP) by NAIN3 with a short incubation. The cloaked sgRNAs were delivered to the GFP-positive HeLa cells using charge-altering releasable transporters resulting in inactive DNA cleavage activity (as measured by GFP fluorescence) in live cells. After the treatment of 5 mM tris(hydroxypropyl)phosphine (THPP) or 1 mM diphenylphosphinobenzene-3-sulfonate (TPPMS) at 37°C, the intracellular DNA cleavage ability of sgRNA was efficiently restored with a maximal level of 81% recovery achieved at the time point of 6 h incubation.

To improve the reversal rate and yield of the de-acylation of caged RNAs, Park et al. designed another type of acylating reagent using quinone methide (QM) elimination for RNA recovery[69] (Figure 3D). The half-life of de-acylation was less than 1h using 0.5 mM TPPMS *in vitro* for azido-QM compound acylated RNAs. The applicability of this method was demonstrated by regulating eGFP mRNA translation in cells.

Other chemical uncaging methods have recently been reported to regulate RNA functions via the 2′-OH group in cells. Ji et al.[70] developed isonitrile-tetrazine click-and-release chemistry to control RNA-guided CRISPR-Cas9 gene editing in human cells. Guide RNA was first caged with isocyanopropyl-carbonate groups via 2′-OH acylation. After transfection, the guide RNA was activated by tetrazine induced cycloadditon and self-elimination of caging groups, restoring gene editing function in cells. An aryl pinacol boronic ester group was another caging group installed at RNA 2′-OH position via acylation.[71] The caging group was removed by hydrogen peroxide for guide RNA activation, again enabling control of CRISPR.

An approach distinct from chemically activated RNA uncaging, light-triggered photocaging enables precise spatial and temporal control of RNA activity. Velema et al.[21] designed "photocloaking" agents which contain a photolabile *ortho*-nitroveratryl group and an active carbamate group that can react with the 2′-OH groups of RNA (Figure 3E). The capability of using this strategy for optochemical control of RNA in a cellular environment was assessed with a 237nt RNA construct encoding dimeric Broccoli aptamers whose folded structure can bind DFHBI dye and generate fluorescence (Figure 3F). The *in vitro* photocloaked RNA aptamer was transfected into HeLa cells. This resulted in no fluorescence until cells were exposed to 365 nm light for 30 min, restoring Broccoli RNA aptamer fluorescence.

SITE-DIRECTED LABELING OF RNA VIA 2′-OH GROUP FOR IN-CELL TRACKING

Selective functionalization of RNA is one of the most important chemical strategies to enable analysis of transcriptome biology. Hydroxyl groups can be an important site for modifying RNA via solid-phase synthesis with high levels of control.[65,72] The modified nucleosides are either *de novo* synthesized or commercially available with alkyne groups attached at 2′-*O*-position. However, this total chemical synthesis technology is limited to relatively short RNAs, is costly from commercial sources, and can be inaccessible to nonspecialist laboratories.

The possibility of post-synthetic labeling of RNA with hydroxyl groups (2′-OH, 3′-OH) was hinted at by early studies of Hiratsuka and coworkers.[73,74] They synthesized fluorescent mononucleotide (ATP and GTP) analogs by reacting with an excess of isatoic anhydrides (e.g., NMIA) in water, yielding solvatochromic fluorescence. More recently, researchers were inspired to label the 2′-OH group of whole RNA strands, developing new reagents with increased solubility, tuned reactivity, and different functional groups, such as biotin-containing anhydrides,[75,76] tertiary-amine-containing anhydride,[77] alkyne,[77,78] or azide-containing acylimidazoles.[66,79] Although they can be efficient, these stochastic polyacylation-based labeling methods are relatively nonselective along the RNA strand, placing limits on applications, especially for cellular RNA study.

To address this challenge, new strategies have been developed to site-selectively introduce modification to the 2′-OH group of RNA by localized acylation. Kool and coworkers[80] developed a DNA-assisted method for site-directed acylation of RNAs. The method, RNA acylation at induced loops (RAIL), utilizes the low reactivity of acylating reagent NAIN3 in a double-stranded structure with complementary DNA to protect all but the desired reaction sites in an RNA; the complementary DNA omits one or more complementary nucleotides to induce

Figure 3. RNA caging strategies employing post-transcriptional reaction at 2′-OH groups

(A) General approach for RNA caging and on-demand activation in cells. The appended group (red) can be designed to respond to chemical inducers or to light.

(B) Reactions involved in chemically activated RNA caging through polyacylation ("cloaking") of RNA with NAIN3. The structures of some water-soluble phosphines (R_3P) for removal of NAIN3 are shown.

(C) Application of phosphine-activated RNA 2′-OH caging strategy to regulate CRISPR-cas9 gene editing inside cells.

(D) A faster-reacting quinone-methide (QM) design for phosphine-activated uncaging in cells. Error bars: standard deviation of triplicate samples; p values: "****" $p < 0.001$, "***" $p < 0.01$, "*" $p < 0.05$, "ns." not significant.

(E) Structure of light-activated "photocloaking" reagents (PCAs) and the reaction scheme of RNA 2′-OH acylation and light-triggered deacylation to restore RNA function.

(F) Application of light-activated RNA 2′-OH caging strategy to regulate the function of a fluorogenic aptamer in cells.

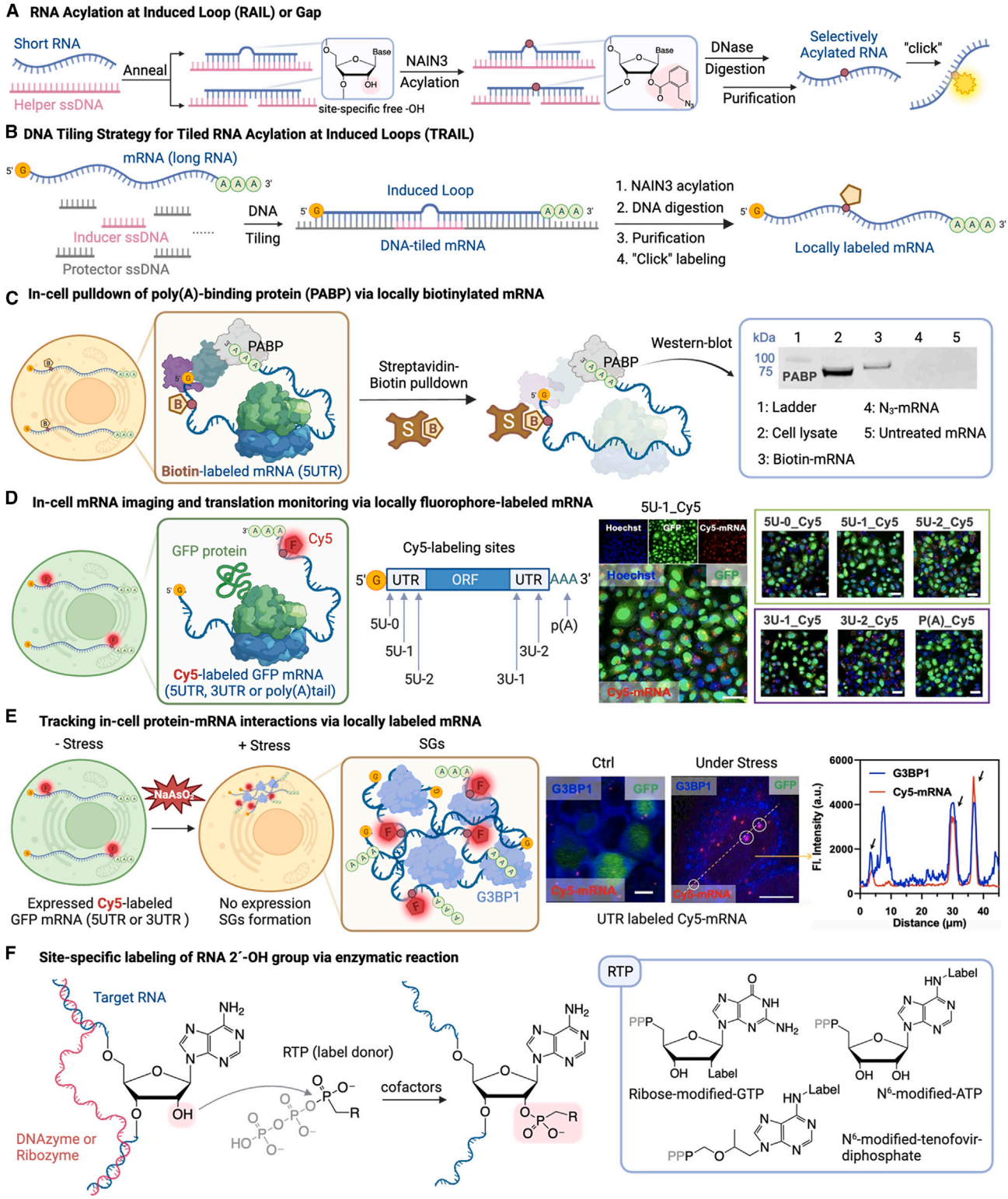

Figure 4. Strategies for modifying 2′-OH groups at local sites in RNA

(A) RNA acylation at induced loops (RAIL) or gaps is used for site-directed RNA labeling using a 2′-OH-reactive reagent that prefers RNA loops over RNA in duplex structures.

(B) For longer RNAs, tiled RNA acylation at induced loops (TRAIL) has been developed to modify specific sites in mRNAs.

(C) In-cell pull-down application of an mRNA locally biotinylated in the 5′-UTR region via TRAIL method.

(legend continued on next page)

a small RNA loop of high reactivity.[29] Alternatively, two oligomers were hybridized along the RNA, leaving a reactive gap in the RNA between them (Figure 4A). In tests, NAIN3 was used to react with RNA in the DNA-RNA assembly, followed by DNase treatment and ethanol precipitation to recover modified RNAs. The results showed that high-yield 2′-OH acylation could be achieved at a predetermined site in the RNA. The applicability of the RAIL method was demonstrated by controlling of an 81nt tandem hammerhead ribozyme, and by dual-labeling a 65nt small nucleolar RNA, SNORD78, for FRET experiments.

Encouraged by the site-directed acylation of short RNA, Xiao et al. extended the method for RNAs too long to be covered by a single DNA oligonucleotide and applied it to intracellular function. TRAIL (tiled RNA acylation at induced loops) was described as a method for mRNA conjugation utilizing a DNA-tiling strategy.[81] Researchers employed a pool of inexpensive "protector" DNAs to hybridize and block the undesired 2′-OH groups in mRNA combined with an "inducer" DNA to extrude a reactive loop for acylation at a desired site (Figure 4B). mRNA and DNA pool were first annealed with a 1:2 ratio, followed by acylation with NAIN3. DNase treatment efficiently removed the helper DNAs, and the modified mRNA was purified by RNA spin column. Gel analysis and qPCR experiments showed that mRNA could be selectively acylated at the looped-out nucleotides in different regions, including untranslated regions (UTRs), poly(A) tail, and open reading frame (ORF), with 60–70% acylation yield. The precise acylation within the coding region of an mRNA enabled the suppression of mRNA expression and led to specific ribosome stalling. Acylation in the 5′-UTR region with a biotin group enabled pull-down of mRNA-associated proteins from cell lysates (Figure 4C). Introducing a fluorophore into the 5′-UTR, 3′-UTR, or poly(A) tail of GFP mRNA, they achieved efficient mRNA imaging and tracking of RNA-protein interactions in HeLa cells (Figures 4D and 4E).

In addition to chemical acylation, the 2′-OH group can also be site-specifically labeled through enzymatic labeling (Figure 4F). The Höbartner group has evolved a set of DNAzymes[82] and ribozymes[83,84] via *in vitro* selection that can efficiently label the 2′-OH group of a specific adenosine in RNA with the help of different label donors including ribose-modified GTP, N^6-modified ATP, and N^6-modified tenofovir-diphosphate. If cell-permeable label donors can be developed, the application holds promise for labeling RNA in cells in the future.

PROFILING SMALL MOLECULE INTERACTIONS

Several experimental approaches have been developed that use 2′-OH reactive chemical probes to identify RNA interactions of small molecules (e.g., riboswitch ligands, investigational and FDA-approved drugs). These approaches can be categorized as indirect or direct; indirect approaches look for changes in the RNA as a result of ligand binding, while direct approaches capture the ligand on RNA where it binds (Figure 5).

Indirect detection of RNA-small molecule interactions

Indirect approaches that interrogate RNA-ligand interactions rely heavily on 2′-OH-based chemical probing of RNA structures (e.g., SHAPE[85] and SHAPE-MaP[86,87]). The central assumption of these approaches is that the binding of small molecules can shield local 2′-OH groups from chemical probing or alter the reactivity toward chemical probing reagents. Thus, a pivotal prerequisite for this detection approach is an accurate, quantitative method to characterize RNA structures at high resolution. Upon drug binding, the altered accessibility and reactivity of 2′-OH groups are typically probed with 2′-OH acylating probes. The resulting covalent 2′-modifications are then detected by deep sequencing as RT-stop signals[85] or correlated mutational signals.[86,87]

To date, most RNA-ligand interactions indirectly detected using RNA structure probing have focused on riboswitches and their ligands *in vitro*, with one reporting on $tRNA^{Asp}$.[85] Riboswitches undergo conformational changes when engaging with cognate ligands, making them highly suitable for RNA structural probing with 2′-OH chemistry (Figure 5A). An early SHAPE analysis revealed that small-molecule fragments can induce an alternative conformation of the TPP riboswitch, which is inaccessible by its cognate ligand.[88] Recent advancements in SHAPE-MaP combined with fragment-based ligand discovery led to the discovery of small molecules binding to distinct but closely located subsites in the TPP riboswitch.[86,87] Other *in vitro* studies reported on cotranscriptional SHAPE-seq, coupling *in vitro* RNAP arrest with high-throughput structure probing to explore ligand-induced alternative riboswitch conformations during cotranscriptional folding.[89–91] These RNA structure probing approaches collectively demonstrated the capability of this indirect approach to detect RNA binding sites and ligandable RNA structure dynamics when integrated with high-throughput strategies.

A limited number of studies have attempted to characterize RNA-small molecule binding in cells with indirect 2′-OH-based RNA structure probing techniques. Weeks and Pielak et al. used the acylating reagent 1M7 to probe the ligand-bound and unbound states of the adenine riboswitch in *E. coli* cells.[92] Treatment of live *E. coli* with riboswitch ligand 2AP induced localized changes in SHAPE reactivity in the binding pocket, confirming that 2AP binding affects the local RNA structure. This study highlights the power of RNA structural probing in characterizing RNA-small molecule engagement. Although powerful, the detection of small molecule binding across the entire transcriptome with such indirect 2′-OH chemistry-based RNA structure probing has yet to be reported. One potential hurdle of such approaches is that the background of structure probing signals is high, potentially obscuring drug-induced changes. In addition, while

(D) Application of TRAIL to mRNA simultaneous imaging and translation via locally fluorophore-labeled mRNA. Red: Cy5-mRNA, green: GFP protein, blue: Hoechst-stained nucleus.
(E) In-cell tracking of mRNA-protein interaction vial TRAIL-labeled mRNA with Cy5 fluorophore at UTR region. Cell imaging was performed to monitor the location and expression of Cy5-labeled mRNA under normal conditions and under stress, in stress granules (SGs). Red: Cy5-mRNA, green: GFP protein, blue: G3BP1-labeled SGs. Scale bar: 13 μm.
(F) Scheme of enzyme-catalyzed site-specific labeling of RNA 2′-OH groups developed by Höbartner and coworkers. The structures of employed label donors are shown.

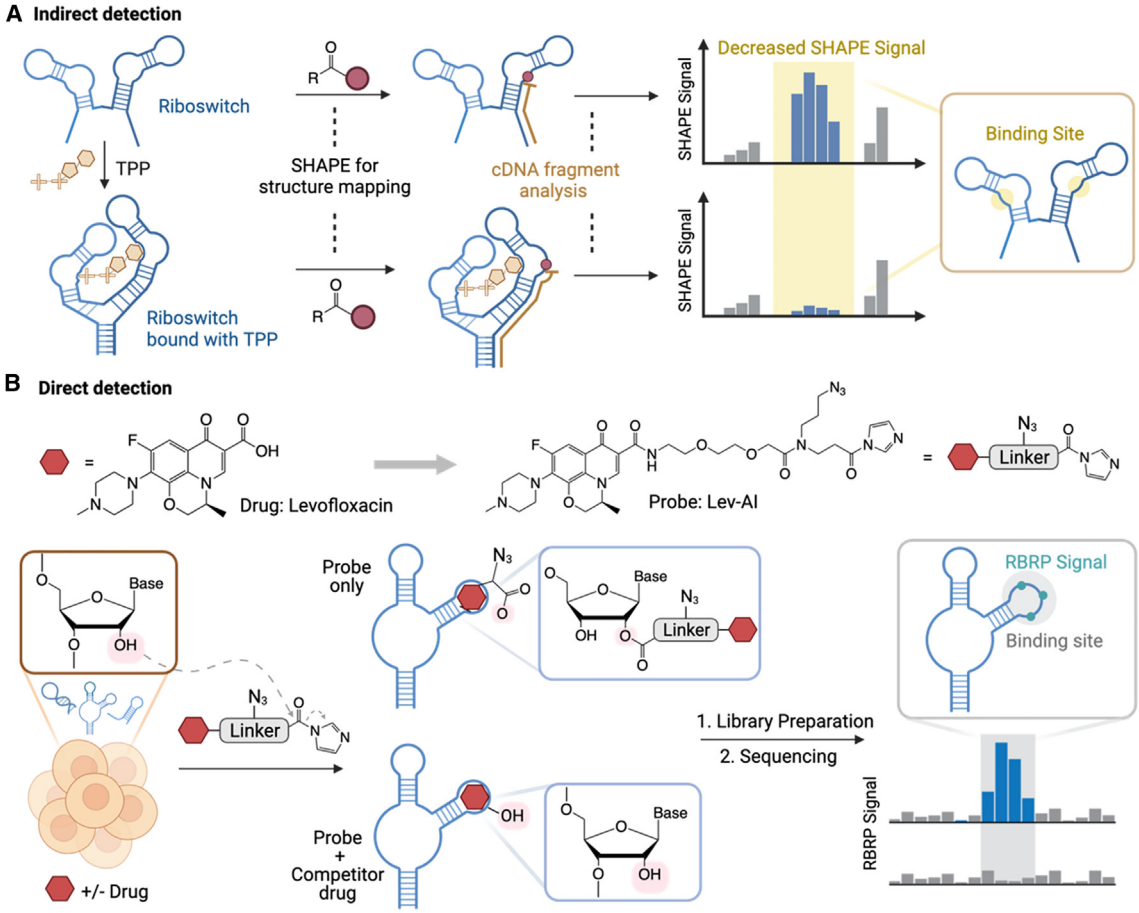

Figure 5. Strategies for using 2′-OH reactivity to profile small molecule interactions with RNA in intact cells

(A) Indirect detection employs SHAPE reagents to probe differences in RNA structure of bound and unbound states as a result of small molecule binding.

(B) Direct detection of RNA-small molecule interactions employs a small molecule probe with an acylating warhead attached. Cells are treated with the acylating probe in the presence or absence of the competing unmodified small molecule. The acylating probe marks its binding sites by reacting at 2′-OH groups nearby, and the sites are identified via reverse transcription stops and enrichment, analyzed by deep sequencing.

riboswitch RNAs evolved to undergo structural transitions, some ligands may induce relatively little change in the underlying structure of non-riboswitch RNAs.

Direct detection of RNA-small molecule interactions

Direct approaches rely on the derivatization of small molecules with RNA-reactive warheads that covalently modify local nucleotides (Figure 5B). The main assumption of these approaches involving the 2′-OH handle is that the binding of small molecules can promote nearby hydroxyls to react with the RNA-reactive warheads (e.g., acylimidazoles), hence allowing direct trapping of the drug locally on the RNA. Importantly, such chemical probes can contain "click" handles, which can be coupled with next-generation sequencing to analyze the entire transcriptome. Two independent studies recently reported experimental methods based on 2′-OH chemistry to interrogate RNA-drug binding. It should also be noted that related chemical trapping methods for direct mapping of RNA-small molecule interactions make use of electrophiles that react with RNA bases; nitrogen mustard- or diazirine-conjugated ligand analogs are used in this approach.[14,93]

RNA-ligand binding sites can be probed directly by measuring proximity-promoted 2′-acylation with acylimidazole-conjugates of small-molecule drugs (Figure 5B). For example, the reactivity-based RNA profiling (RBRP) approach was recently reported and used in cells to unravel transcriptome-wide binding sites of US Food and Drug Administration (FDA)-approved drugs.[94] The RBRP approach involves the use of cell-permeable RNA 2′-OH acylation probes (functionalized drug analogs that contain acylimidazole-substituted linkers to react at RNA 2′-OH groups) to pinpoint and quantify off-target RNA interactions of protein-targeted drugs transcriptome-wide. The binding of an acylimidazole conjugate of a drug to intracellular RNAs promotes enriched acylation of 2′-OH groups near the drug binding sites. RNA drug-binding sites thus have greater numbers of reverse transcriptase (RT) stops, which are enriched by biotin-mediated pull-down and competition with the unmodified drug. These drug-promoted acylations were identified with a modified *in vivo* RNA mapping protocol, allowing precise identification of small molecule binding locations within the entire intracellular RNA population. RBRP showed that three FDA-approved protein-targeted drugs pervasively interact with the

human transcriptome, and such off-target interactions can cause unintended biological effects on intracellular RNAs. For example, the antibiotic drug Levofloxacin can engage with a G-quadruplex structure in the 5′ UTR of YBX1 mRNA, which suppresses translation of YBX1 mRNA both *in vitro* and in live HEK293 cells. Notably, acylating probes demonstrated nearly equal reactivities toward all four ribonucleotides transcriptome-wide, potentially expanding the scope of RNA sequences scouted for ligand-binding sites. This contrasts with diazirine-based profiling methods that display substantial labeling biases toward guanine nucleobase.

Another recent study used 2′-OH acylation probes to detect small-molecule binding sites in SARS-CoV-2 5′ UTR *in vitro*.[95] Chemical-guided selective 2′-hydroxyl acylation analyzed by primer extension (cgSHAPE) applies a similar principle as RBRP to detect RNA ligand binding sites *in vitro*; specifically, 2′-OH acylating probe (drug analog functionalized with furoyl acylimidazole) promotes enriched 2′-acylation at the ligand binding sites, which cause readthrough mutations during reverse transcription that can be detected by RNA sequencing. cgSHAPE identifies a bulged G in SARS-CoV-2 5′ UTR as the primary binding site by a coumarin derivative. Furthermore, the replacement of acylimidazole moiety in the cgSHAPE probe with a ligand that recruits ribonuclease L rendered RiboTAC molecules that degrade SARS-CoV-2 RNA *in vitro* and in cells.

This type of direct approach has substantial potential for probing the chemical space of RNA-interacting ligands and characteristics that define a ligandable RNA pocket. The main limitation of such an approach is that RNA-reactive warheads are designed to identify nucleotides that are structurally accessible and flexible. RNA-small molecule binding loci that are highly base-paired or shielded by other cellular components (proteins and/or RNA) may be challenging to detect. Combining these approaches with other orthogonal methods for RNA-ligand profiling could provide a comprehensive view of drug interactions transcriptome-wide.

CONCLUSIONS AND FUTURE PROSPECTS

The chemical modification and profiling of RNAs through the reaction of 2′-OH groups presents exciting opportunities for studying intracellular RNAs for both basic science and biomedical applications. The fact that this group is present along the entire strand highlights the potential for probing and modifying RNAs at any position in the biopolymer, and the ubiquity of this group enables researchers to address RNAs transcriptome-wide. The ongoing development of a broad range of tunable chemical reagents enables applicability ranging from trace-level reactions for probing structure and interactions to high-yield reactions that enable caging, conjugation, and protection. The advancement of SHAPE mapping technologies and the recent introduction of crosslinking strategies using 2′-OH handles have contributed significantly to the investigation of RNA 2D/3D structures and the RNA interactome within cells. The high-yield acylation of 2′-OH groups with designer acylating reagents enables effective chemical and optical regulation of RNA functions in cellular contexts. Reactions at 2′-OH can be carried out either stochastically along the length of the strand or in a site-directed manner, depending on the intended application. Additionally, the profiles of intracellular RNA-small molecule interactions can be explored through 2′-OH chemistry, offering insights into targeted and off-target interactions of drugs in the transcriptome, and enabling the identification of ligandable RNA pockets for future biomedical studies.

Many opportunities exist for future development of 2′-OH-directed chemistries for intracellular applications. For example, it may be possible to develop more selective tuned probes and warheads that react with specific structures and targets. One pathway to address this may be to identify OH-reactive groups that are more selective for RNA and less reactive with water. A second avenue may be the identification of specific folded RNA structures that have unusually high reactivity; for example, chiral reagents might take advantage of the macrochirality of RNA,[96] matching small molecule chirality with the biopolymer handedness to yield better reactions with lower background. A third opportunity with broad applications will lie in the development of *in vitro* 2′-*O*-modified RNAs that are then introduced into cells to modulate lifetimes or gene expression.[22] Finally, 2′-OH-reactive warheads could enable the broader study of small molecule interactions in the transcriptome. This could uncover new information about, for example, intracellular metabolites, and also could be used to discover new ligands for specific intracellular RNAs.

ACKNOWLEDGMENTS

We thank the U.S. National Institutes of Health (GM145357) for support.

DECLARATION OF INTERESTS

The authors declare no competing interests.

REFERENCES

1. Sonneveld, S., Verhagen, B.M.P., and Tanenbaum, M.E. (2020). Heterogeneity in mRNA Translation. Trends Cell Biol. *30*, 606–618. https://doi.org/10.1016/j.tcb.2020.04.008.

2. Cech, T.R., and Steitz, J.A. (2014). The noncoding RNA revolution-trashing old rules to forge new ones. Cell *157*, 77–94. https://doi.org/10.1016/j.cell.2014.03.008.

3. Ganser, L.R., Kelly, M.L., Herschlag, D., and Al-Hashimi, H.M. (2019). The roles of structural dynamics in the cellular functions of RNAs. Nat. Rev. Mol. Cell Biol. *20*, 474–489. https://doi.org/10.1038/s41580-019-0136-0.

4. Kapranov, P., and St Laurent, G. (2012). Dark Matter RNA: Existence, Function, and Controversy. Front. Genet. *3*, 60. https://doi.org/10.3389/fgene.2012.00060.

5. Lieberman, J. (2018). Tapping the RNA world for therapeutics. Nat. Struct. Mol. Biol. *25*, 357–364. https://doi.org/10.1038/s41594-018-0054-4.

6. Booth, B.J., Nourreddine, S., Katrekar, D., Savva, Y., Bose, D., Long, T.J., Huss, D.J., and Mali, P. (2023). RNA editing: Expanding the potential of RNA therapeutics. Mol. Ther. *31*, 1533–1549. https://doi.org/10.1016/j.ymthe.2023.01.005.

7. Conti, B.A., and Oppikofer, M. (2022). Biomolecular condensates: new opportunities for drug discovery and RNA therapeutics. Trends Pharmacol. Sci. *43*, 820–837. https://doi.org/10.1016/j.tips.2022.07.001.

8. Dykstra, P.B., Kaplan, M., and Smolke, C.D. (2022). Engineering synthetic RNA devices for cell control. Nat. Rev. Genet. *23*, 215–228. https://doi.org/10.1038/s41576-021-00436-7.

9. Wissink, E.M., Vihervaara, A., Tippens, N.D., and Lis, J.T. (2019). Nascent RNA analyses: tracking transcription and its regulation. Nat. Rev. Genet. *20*, 705–723. https://doi.org/10.1038/s41576-019-0159-6.

10. Klöcker, N., Weissenboeck, F.P., and Rentmeister, A. (2020). Covalent labeling of nucleic acids. Chem. Soc. Rev. *49*, 8749–8773. https://doi.org/10.1039/d0cs00600a.

11. Hafner, M., Landthaler, M., Burger, L., Khorshid, M., Hausser, J., Berninger, P., Rothballer, A., Ascano, M., Jr., Jungkamp, A.C., Munschauer, M., et al. (2010). Transcriptome-wide identification of RNA-binding protein and microRNA target sites by PAR-CLIP. Cell *141*, 129–141. https://doi.org/10.1016/j.cell.2010.03.009.

12. Velema, W.A., and Lu, Z. (2023). Chemical RNA Cross-Linking: Mechanisms, Computational Analysis, and Biological Applications. Jacs Au *3*, 316–332. https://doi.org/10.1021/jacsau.2c00625.

13. Qiu, Z., Lu, L., Jian, X., and He, C. (2008). A diazirine-based nucleoside analogue for efficient DNA interstrand photocross-linking. J. Am. Chem. Soc. *130*, 14398–14399. https://doi.org/10.1021/ja805445j.

14. Tong, Y., Gibaut, Q.M.R., Rouse, W., Childs-Disney, J.L., Suresh, B.M., Abegg, D., Choudhary, S., Akahori, Y., Adibekian, A., Moss, W.N., and Disney, M.D. (2022). Transcriptome-Wide Mapping of Small-Molecule RNA-Binding Sites in Cells Informs an Isoform-Specific Degrader of QSOX1 mRNA. J. Am. Chem. Soc. *144*, 11620–11625. https://doi.org/10.1021/jacs.2c01929.

15. Tijerina, P., Mohr, S., and Russell, R. (2007). DMS footprinting of structured RNAs and RNA-protein complexes. Nat. Protoc. *2*, 2608–2623. https://doi.org/10.1038/nprot.2007.380.

16. Weng, X., Gong, J., Chen, Y., Wu, T., Wang, F., Yang, S., Yuan, Y., Luo, G., Chen, K., Hu, L., et al. (2020). Keth-seq for transcriptome-wide RNA structure mapping. Nat. Chem. Biol. *16*, 489–492. https://doi.org/10.1038/s41589-019-0459-3.

17. Merino, E.J., Wilkinson, K.A., Coughlan, J.L., and Weeks, K.M. (2005). RNA structure analysis at single nucleotide resolution by selective 2 '-hydroxyl acylation and primer extension (SHAPE). J. Am. Chem. Soc. *127*, 4223–4231. https://doi.org/10.1021/ja043822v.

18. Velikyan, I., Acharya, S., Trifonova, A., Földesi, A., and Chattopadhyaya, J. (2001). The pK(a)'s of 2'-hydroxyl group in nucleosides and nucleotides. J. Am. Chem. Soc. *123*, 2893–2894. https://doi.org/10.1021/ja0036312.

19. Jash, B., and Kool, E.T. (2022). Conjugation of RNA via 2'-OH acylation: Mechanisms determining nucleotide reactivity. Chem. Commun. *58*, 3693–3696. https://doi.org/10.1039/d2cc00660j.

20. Velema, W.A., and Kool, E.T. (2020). The chemistry and applications of RNA 2 '-OH acylation. Nat. Rev. Chem *4*, 22–37. https://doi.org/10.1038/s41570-019-0147-6.

21. Velema, W.A., Kietrys, A.M., and Kool, E.T. (2018). RNA Control by Photoreversible Acylation. J. Am. Chem. Soc. *140*, 3491–3495. https://doi.org/10.1021/jacs.7b12408.

22. Fang, L., Xiao, L., Jun, Y.W., Onishi, Y., and Kool, E.T. (2023). Reversible 2'-OH acylation enhances RNA stability. Nat. Chem. *15*, 1296–1305. https://doi.org/10.1038/s41557-023-01246-6.

23. Watters, K.E., and Lucks, J.B. (2016). Mapping RNA Structure In Vitro with SHAPE Chemistry and Next-Generation Sequencing (SHAPE-Seq). Methods Mol. Biol. *1490*, 135–162. https://doi.org/10.1007/978-1-4939-6433-8_9.

24. Busan, S., Weidmann, C.A., Sengupta, A., and Weeks, K.M. (2019). Guidelines for SHAPE Reagent Choice and Detection Strategy for RNA Structure Probing Studies. Biochemistry-Us *58*, 2655–2664. https://doi.org/10.1021/acs.biochem.8b01218.

25. Salari, R., Kimchi-Sarfaty, C., Gottesman, M.M., and Przytycka, T.M. (2013). Sensitive measurement of single-nucleotide polymorphism-induced changes of RNA conformation: application to disease studies. Nucleic Acids Res. *41*, 44–53. https://doi.org/10.1093/nar/gks1009.

26. Spitale, R.C., Flynn, R.A., Torre, E.A., Kool, E.T., and Chang, H.Y. (2014). RNA structural analysis by evolving SHAPE chemistry. Wires Rna *5*, 867–881. https://doi.org/10.1002/wrna.1253.

27. Boerneke, M.A., Ehrhardt, J.E., and Weeks, K.M. (2019). Physical and Functional Analysis of Viral RNA Genomes by SHAPE. Annu. Rev. Virol. *6*, 93–117. https://doi.org/10.1146/annurev-virology-092917-043315.

28. McGinnis, J.L., Dunkle, J.A., Cate, J.H.D., and Weeks, K.M. (2012). The mechanisms of RNA SHAPE chemistry. J. Am. Chem. Soc. *134*, 6617–6624. https://doi.org/10.1021/ja2104075.

29. Xiao, L., Fang, L., and Kool, E.T. (2022). Acylation probing of "generic" RNA libraries reveals critical influence of loop constraints on reactivity. Cell Chem. Biol. *29*, 1341–1352.e8. https://doi.org/10.1016/j.chembiol.2022.05.005.

30. Mortimer, S.A., and Weeks, K.M. (2007). A fast-acting reagent for accurate analysis of RNA secondary and tertiary structure by SHAPE chemistry. J. Am. Chem. Soc. *129*, 4144–4145. https://doi.org/10.1021/ja0704028.

31. Deigan, K.E., Li, T.W., Mathews, D.H., and Weeks, K.M. (2009). Accurate SHAPE-directed RNA structure determination. Proc. Natl. Acad. Sci. USA *106*, 97–102. https://doi.org/10.1073/pnas.0806929106.

32. Lucks, J.B., Mortimer, S.A., Trapnell, C., Luo, S., Aviran, S., Schroth, G.P., Pachter, L., Doudna, J.A., and Arkin, A.P. (2011). Multiplexed RNA structure characterization with selective 2'-hydroxyl acylation analyzed by primer extension sequencing (SHAPE-Seq). Proc. Natl. Acad. Sci. USA *108*, 11063–11068. https://doi.org/10.1073/pnas.1106501108.

33. Spitale, R.C., Crisalli, P., Flynn, R.A., Torre, E.A., Kool, E.T., and Chang, H.Y. (2013). RNA SHAPE analysis in living cells. Nat. Chem. Biol. *9*, 18–20. https://doi.org/10.1038/Nchembio.1131.

34. Yang, M., Woolfenden, H.C., Zhang, Y., Fang, X., Liu, Q., Vigh, M.L., Cheema, J., Yang, X., Norris, M., Yu, S., et al. (2020). Intact RNA structurome reveals mRNA structure-mediated regulation of miRNA cleavage *in vivo*. Nucleic Acids Res. *48*, 8767–8781. https://doi.org/10.1093/nar/gkaa577.

35. Yang, X., Cheema, J., Zhang, Y., Deng, H., Duncan, S., Umar, M.I., Zhao, J., Liu, Q., Cao, X., Kwok, C.K., and Ding, Y. (2020). RNA G-quadruplex structures exist and function *in vivo* in plants. Genome Biol. *21*, 226. https://doi.org/10.1186/s13059-020-02142-9.

36. Siegfried, N.A., Busan, S., Rice, G.M., Nelson, J.A.E., and Weeks, K.M. (2014). RNA motif discovery by SHAPE and mutational profiling (SHAPE-MaP). Nat. Methods *11*, 959–965. https://doi.org/10.1038/nmeth.3029.

37. Smola, M.J., Rice, G.M., Busan, S., Siegfried, N.A., and Weeks, K.M. (2015). Selective 2'-hydroxyl acylation analyzed by primer extension and mutational profiling (SHAPE-MaP) for direct, versatile and accurate RNA structure analysis. Nat. Protoc. *10*, 1643–1669. https://doi.org/10.1038/nprot.2015.103.

38. Guo, L.T., Adams, R.L., Wan, H., Huston, N.C., Potapova, O., Olson, S., Gallardo, C.M., Graveley, B.R., Torbett, B.E., and Pyle, A.M. (2020). Sequencing and Structure Probing of Long RNAs Using MarathonRT: A Next-Generation Reverse Transcriptase. J. Mol. Biol. *432*, 3338–3352. https://doi.org/10.1016/j.jmb.2020.03.022.

39. England, W.E., Garfio, C.M., and Spitale, R.C. (2021). Chemical Approaches To Analyzing RNA Structure Transcriptome-Wide. Chembiochem *22*, 1114–1121. https://doi.org/10.1002/cbic.202000340.

40. McGinnis, J.L., Liu, Q., Lavender, C.A., Devaraj, A., McClory, S.P., Fredrick, K., and Weeks, K.M. (2015). In-cell SHAPE reveals that free 30S ribosome subunits are in the inactive state. Proc. Natl. Acad. Sci. USA *112*, 2425–2430. https://doi.org/10.1073/pnas.1411514112.

41. Watters, K.E., Abbott, T.R., and Lucks, J.B. (2016). Simultaneous characterization of cellular RNA structure and function with in-cell SHAPE-Seq. Nucleic Acids Res. *44*, e12. https://doi.org/10.1093/nar/gkv879.

42. Smola, M.J., Christy, T.W., Inoue, K., Nicholson, C.O., Friedersdorf, M., Keene, J.D., Lee, D.M., Calabrese, J.M., and Weeks, K.M. (2016). SHAPE reveals transcript-wide interactions, complex structural domains, and protein interactions across the Xist lncRNA in living cells. Proc. Natl. Acad. Sci. USA *113*, 10322–10327. https://doi.org/10.1073/pnas.1600008113.

43. Mustoe, A.M., Busan, S., Rice, G.M., Hajdin, C.E., Peterson, B.K., Ruda, V.M., Kubica, N., Nutiu, R., Baryza, J.L., and Weeks, K.M. (2018). Pervasive Regulatory Functions of mRNA Structure Revealed by High-Resolution SHAPE Probing. Cell *173*, 181–195.e18. https://doi.org/10.1016/j.cell.2018.02.034.

44. Manfredonia, I., Nithin, C., Ponce-Salvatierra, A., Ghosh, P., Wirecki, T.K., Marinus, T., Ogando, N.S., Snijder, E.J., van Hemert, M.J., Bujnicki, J.M., and Incarnato, D. (2020). Genome-wide mapping of SARS-CoV-2 RNA

structures identifies therapeutically-relevant elements. Nucleic Acids Res. *48*, 12436–12452. https://doi.org/10.1093/nar/gkaa1053.

45. Yang, S.L., DeFalco, L., Anderson, D.E., Zhang, Y., Aw, J.G.A., Lim, S.Y., Lim, X.N., Tan, K.Y., Zhang, T., Chawla, T., et al. (2021). Comprehensive mapping of SARS-CoV-2 interactions *in vivo* reveals functional virus-host interactions. Nat. Commun. *12*, 5113. https://doi.org/10.1038/s41467-021-25357-1.

46. Guo, S.K., Nan, F., Liu, C.X., Yang, L., and Chen, L.L. (2021). Mapping circular RNA structures in living cells by SHAPE-MaP. Methods *196*, 47–55. https://doi.org/10.1016/j.ymeth.2021.01.011.

47. Aw, J.G.A., Lim, S.W., Wang, J.X., Lambert, F.R.P., Tan, W.T., Shen, Y., Zhang, Y., Kaewsapsak, P., Li, C., Ng, S.B., et al. (2021). Determination of isoform-specific RNA structure with nanopore long reads. Nat. Biotechnol. *39*, 336–346. https://doi.org/10.1038/s41587-020-0712-z.

48. Yang, M., Zhu, P., Cheema, J., Bloomer, R., Mikulski, P., Liu, Q., Zhang, Y., Dean, C., and Ding, Y. (2022). *In vivo* single-molecule analysis reveals COOLAIR RNA structural diversity. Nature *609*, 394–399. https://doi.org/10.1038/s41586-022-05135-9.

49. Spitale, R.C., Flynn, R.A., Zhang, Q.C., Crisalli, P., Lee, B., Jung, J.W., Kuchelmeister, H.Y., Batista, P.J., Torre, E.A., Kool, E.T., and Chang, H.Y. (2015). Structural imprints *in vivo* decode RNA regulatory mechanisms. Nature *519*, 486–490. https://doi.org/10.1038/nature14263.

50. Sun, L., Fazal, F.M., Li, P., Broughton, J.P., Lee, B., Tang, L., Huang, W., Kool, E.T., Chang, H.Y., and Zhang, Q.C. (2019). RNA structure maps across mammalian cellular compartments. Nat. Struct. Mol. Biol. *26*, 322–330. https://doi.org/10.1038/s41594-019-0200-7.

51. Sun, L., Li, P., Ju, X., Rao, J., Huang, W., Ren, L., Zhang, S., Xiong, T., Xu, K., Zhou, X., et al. (2021). *In vivo* structural characterization of the SARS-CoV-2 RNA genome identifies host proteins vulnerable to repurposed drugs. Cell *184*, 1865–1883.e20. https://doi.org/10.1016/j.cell.2021.02.008.

52. Luo, Q.J., Zhang, J., Li, P., Wang, Q., Zhang, Y., Roy-Chaudhuri, B., Xu, J., Kay, M.A., and Zhang, Q.C. (2021). RNA structure probing reveals the structural basis of Dicer binding and cleavage. Nat. Commun. *12*, 3397. https://doi.org/10.1038/s41467-021-23607-w.

53. Wang, J., Zhang, T., Yu, Z., Tan, W.T., Wen, M., Shen, Y., Lambert, F.R.P., Huber, R.G., and Wan, Y. (2021). Genome-wide RNA structure changes during human neurogenesis modulate gene regulatory networks. Mol. Cell *81*, 4942–4953.e8. https://doi.org/10.1016/j.molcel.2021.09.027.

54. Cao, J., and Xue, Y. (2021). Characteristic chemical probing patterns of loop motifs improve prediction accuracy of RNA secondary structures. Nucleic Acids Res. *49*, 4294–4307. https://doi.org/10.1093/nar/gkab250.

55. Marinus, T., Fessler, A.B., Ogle, C.A., and Incarnato, D. (2021). A novel SHAPE reagent enables the analysis of RNA structure in living cells with unprecedented accuracy. Nucleic Acids Res. *49*, e34. https://doi.org/10.1093/nar/gkaa1255.

56. Xiao, L., Fang, L., Chatterjee, S., and Kool, E.T. (2023). Diverse Reagent Scaffolds Provide Differential Selectivity of 2'-OH Acylation in RNA. J. Am. Chem. Soc. *145*, 143–151. https://doi.org/10.1021/jacs.2c09040.

57. Stephenson, W., Razaghi, R., Busan, S., Weeks, K.M., Timp, W., and Smibert, P. (2022). Direct detection of RNA modifications and structure using single-molecule nanopore sequencing. Cell Genom. *2*, 100097. https://doi.org/10.1016/j.xgen.2022.100097.

58. Velema, W.A., Park, H.S., Kadina, A., Orbai, L., and Kool, E.T. (2020). Trapping Transient RNA Complexes by Chemically Reversible Acylation. Angew. Chem. Int. Ed. Engl. *59*, 22017–22022. https://doi.org/10.1002/anie.202010861.

59. Van Damme, R., Li, K., Zhang, M., Bai, J., Lee, W.H., Yesselman, J.D., Lu, Z., and Velema, W.A. (2022). Chemical reversible crosslinking enables measurement of RNA 3D distances and alternative conformations in cells. Nat. Commun. *13*, 911. https://doi.org/10.1038/s41467-022-28602-3.

60. Christy, T.W., Giannetti, C.A., Houlihan, G., Smola, M.J., Rice, G.M., Wang, J., Dokholyan, N.V., Laederach, A., Holliger, P., and Weeks, K.M. (2021). Direct Mapping of Higher-Order RNA Interactions by SHAPE-JuMP. Biochemistry-Us *60*, 1971–1982. https://doi.org/10.1021/acs.biochem.1c00270.

61. Brown, W., Bardhan, A., Darrah, K., Tsang, M., and Deiters, A. (2022). Optical Control of MicroRNA Function in Zebrafish Embryos. J. Am. Chem. Soc. *144*, 16819–16826. https://doi.org/10.1021/jacs.2c04479.

62. Weissenboeck, F.P., Schepers, H., and Rentmeister, A. (2023). Optochemical Control of mRNA Translation in Eukaryotes. Angew. Chem. Int. Ed. Engl. *62*, e202301778. https://doi.org/10.1002/anie.202301778.

63. Ankenbruck, N., Courtney, T., Naro, Y., and Deiters, A. (2018). Optochemical Control of Biological Processes in Cells and Animals. Angew. Chem. Int. Ed. Engl. *57*, 2768–2798. https://doi.org/10.1002/anie.201700171.

64. Knorre, D.G., Pustoshilova, N.M., Teplova, M., and Shamovskiĭ, G.G. (1965). [The production of transfer RNA acetylated by 2'-oxy groups]. Biokhimiia *30*, 1218–1224.

65. Chaulk, S.G., and MacMillan, A.M. (1998). Caged RNA: photo-control of a ribozyme reaction. Nucleic Acids Res. *26*, 3173–3178. https://doi.org/10.1093/nar/26.13.3173.

66. Kadina, A., Kietrys, A.M., and Kool, E.T. (2018). RNA Cloaking by Reversible Acylation. Angew. Chem. Int. Ed. Engl. *57*, 3059–3063. https://doi.org/10.1002/anie.201708696.

67. Habibian, M., McKinlay, C., Blake, T.R., Kietrys, A.M., Waymouth, R.M., Wender, P.A., and Kool, E.T. (2019). Reversible RNA acylation for control of CRISPR-Cas9 gene editing. Chem. Sci. *11*, 1011–1016. https://doi.org/10.1039/c9sc03639c.

68. Wang, S.R., Wu, L.Y., Huang, H.Y., Xiong, W., Liu, J., Wei, L., Yin, P., Tian, T., and Zhou, X. (2020). Conditional control of RNA-guided nucleic acid cleavage and gene editing. Nat. Commun. *11*, 91. https://doi.org/10.1038/s41467-019-13765-3.

69. Park, H.S., Jash, B., Xiao, L., Jun, Y.W., and Kool, E.T. (2021). Control of RNA with quinone methide reversible acylating reagents. Org. Biomol. Chem. *19*, 8367–8376. https://doi.org/10.1039/d1ob01713f.

70. Ji, H., Xiong, W., Guo, S., Wang, S., Xing, X., Tian, T., and Zhou, X. (2023). Isonitrile-Tetrazine Click-and-Release Chemistry for Controlling RNA-Guided Nucleic Acid Cleavage. ACS Chem. Biol. *18*, 1829–1837. https://doi.org/10.1021/acschembio.3c00255.

71. Ji, H., Xiong, W., Zhang, K., Tian, T., and Zhou, X. (2022). Hydrogen Peroxide-triggered Chemical Strategy for Controlling CRISPR systems. Chem. Asian J. *17*, e202200214. https://doi.org/10.1002/asia.202200214.

72. Paredes, E., and Das, S.R. (2011). Click chemistry for rapid labeling and ligation of RNA. Chembiochem *12*, 125–131. https://doi.org/10.1002/cbic.201000466.

73. Hiratsuka, T. (1982). New Fluorescent Analogs of Camp and Cgmp Available as Substrates for Cyclic-Nucleotide Phosphodiesterase. J. Biol. Chem. *257*, 13354–13358.

74. Hiratsuka, T. (1983). New ribose-modified fluorescent analogs of adenine and guanine nucleotides available as substrates for various enzymes. Biochim. Biophys. Acta *742*, 496–508. https://doi.org/10.1016/0167-4838(83)90267-4.

75. Ursuegui, S., Chivot, N., Moutin, S., Burr, A., Fossey, C., Cailly, T., Laayoun, A., Fabis, F., and Laurent, A. (2014). Biotin-conjugated N-methylisatoic anhydride: a chemical tool for nucleic acid separation by selective 2 ' -hydroxyl acylation of RNA. Chem. Commun. *50*, 5748–5751. https://doi.org/10.1039/c4cc01134a.

76. Ursuegui, S., Yougnia, R., Moutin, S., Burr, A., Fossey, C., Cailly, T., Laayoun, A., Laurent, A., and Fabis, F. (2015). A biotin-conjugated pyridine-based isatoic anhydride, a selective room temperature RNA-acylating agent for the nucleic acid separation. Org. Biomol. Chem. *13*, 3625–3632. https://doi.org/10.1039/c4ob02636e.

77. Fessler, A., Garmon, C., Heavey, T., Fowler, A., and Ogle, C. (2017). Water-soluble and UV traceable isatoic anhydride-based reagents for bioconjugation. Org. Biomol. Chem. *15*, 9599–9602. https://doi.org/10.1039/c7ob02377d.

78. Velema, W.A., and Kool, E.T. (2018). Water-Soluble Leaving Group Enables Hydrophobic Functionalization of RNA. Org. Lett. *20*, 6587–6590. https://doi.org/10.1021/acs.orglett.8b02938.

79. Park, H.S., Kietrys, A.M., and Kool, E.T. (2019). Simple alkanoyl acylating agents for reversible RNA functionalization and control. Chem. Commun. *55*, 5135–5138. https://doi.org/10.1039/c9cc01598a.

80. Xiao, L., Habibian, M., and Kool, E.T. (2020). Site-Selective RNA Functionalization via DNA-Induced Structure. J. Am. Chem. Soc. *142*, 16357–16363. https://doi.org/10.1021/jacs.0c06824.

81. Xiao, L., Jun, Y.W., and Kool, E.T. (2021). DNA Tiling Enables Precise Acylation-Based Labeling and Control of mRNA. Angew. Chem., Int. Ed. *60*, 26798–26805. https://doi.org/10.1002/anie.202112106.

82. Büttner, L., Javadi-Zarnaghi, F., and Höbartner, C. (2014). Site-specific labeling of RNA at internal ribose hydroxyl groups: terbium-assisted deoxyribozymes at work. J. Am. Chem. Soc. *136*, 8131–8137. https://doi.org/10.1021/ja503864v.

83. Ghaem Maghami, M., Dey, S., Lenz, A.K., and Höbartner, C. (2020). Repurposing Antiviral Drugs for Orthogonal RNA-Catalyzed Labeling of RNA. Angew. Chem. Int. Ed. Engl. *59*, 9335–9339. https://doi.org/10.1002/anie.202001300.

84. Ghaem Maghami, M., Scheitl, C.P.M., and Höbartner, C. (2019). Direct in Vitro Selection of Trans-Acting Ribozymes for Posttranscriptional, Site-Specific, and Covalent Fluorescent Labeling of RNA. J. Am. Chem. Soc. *141*, 19546–19549. https://doi.org/10.1021/jacs.9b10531.

85. Wang, B., Wilkinson, K.A., and Weeks, K.M. (2008). Complex ligand-induced conformational changes in tRNA(Asp) revealed by single-nucleotide resolution SHAPE chemistry. Biochemistry-Us *47*, 3454–3461. https://doi.org/10.1021/bi702372x.

86. Zeller, M.J., Favorov, O., Li, K., Nuthanakanti, A., Hussein, D., Michaud, A., Lafontaine, D.A., Busan, S., Serganov, A., Aubé, J., and Weeks, K.M. (2022). SHAPE-enabled fragment-based ligand discovery for RNA. Proc. Natl. Acad. Sci. USA *119*, e2122660119. https://doi.org/10.1073/pnas.2122660119.

87. Zeller, M.J., Nuthanakanti, A., Li, K., Aubé, J., Serganov, A., and Weeks, K.M. (2022). Subsite Ligand Recognition and Cooperativity in the TPP Riboswitch: Implications for Fragment-Linking in RNA Ligand Discovery. ACS Chem. Biol. *17*, 438–448. https://doi.org/10.1021/acschembio.1c00880.

88. Warner, K.D., Homan, P., Weeks, K.M., Smith, A.G., Abell, C., and Ferré--D'Amaré, A.R. (2014). Validating fragment-based drug discovery for biological RNAs: lead fragments bind and remodel the TPP riboswitch specifically. Chem. Biol. *21*, 591–595. https://doi.org/10.1016/j.chembiol.2014.03.007.

89. Watters, K.E., Strobel, E.J., Yu, A.M., Lis, J.T., and Lucks, J.B. (2016). Cotranscriptional folding of a riboswitch at nucleotide resolution. Nat. Struct. Mol. Biol. *23*, 1124–1131. https://doi.org/10.1038/nsmb.3316.

90. Strobel, E.J., Cheng, L., Berman, K.E., Carlson, P.D., and Lucks, J.B. (2019). A ligand-gated strand displacement mechanism for ZTP riboswitch transcription control. Nat. Chem. Biol. *15*, 1067–1076. https://doi.org/10.1038/s41589-019-0382-7.

91. Cheng, L., White, E.N., Brandt, N.L., Yu, A.M., Chen, A.A., and Lucks, J.B. (2022). Cotranscriptional RNA strand exchange underlies the gene regulation mechanism in a purine-sensing transcriptional riboswitch. Nucleic Acids Res. *50*, 12001–12018. https://doi.org/10.1093/nar/gkac102.

92. Tyrrell, J., McGinnis, J.L., Weeks, K.M., and Pielak, G.J. (2013). The cellular environment stabilizes adenine riboswitch RNA structure. Biochemistry-Us *52*, 8777–8785. https://doi.org/10.1021/bi401207q.

93. Velagapudi, S.P., Li, Y., and Disney, M.D. (2019). A cross-linking approach to map small molecule-RNA binding sites in cells. Bioorg. Med. Chem. Lett. *29*, 1532–1536. https://doi.org/10.1016/j.bmcl.2019.04.001.

94. Fang, L., Velema, W.A., Lee, Y., Xiao, L., Mohsen, M.G., Kietrys, A.M., and Kool, E.T. (2023). Pervasive transcriptome interactions of protein-targeted drugs. Nat. Chem. *15*, 1374–1383. https://doi.org/10.1038/s41557-023-01309-8.

95. Tang, Z., Hegde, S., Hao, S., Selvaraju, M., Qiu, J., and Wang, J. (2023). Chemical-guided SHAPE sequencing (cgSHAPE-seq) informs the binding site of RNA-degrading chimeras targeting SARS-CoV-2 5' untranslated region. Preprint at bioRxiv. https://doi.org/10.1101/2023.04.03.535453.

96. Shioi, R., Xiao, L., Chatterjee, S., and Kool, E.T. (2023). Stereoselective RNA Reaction with Chiral 2'-OH Acylating Agents. Chem. Sci. https://doi.org/10.1039/d3sc03067a.